and ^{31}P-NMR patterns are as expected.

The reaction of BPPFA with $Fe(CO)_5$ or $Fe_3(CO)_{12}$ afforded two major products **2** and **3**, while the reaction with $Fe_2(CO)_9$ gave **3** alone. The purple unidentified compound that was formed in a trace amount from the reaction with $Fe_3(CO)_{12}$ (see Experimental) may be considered as a trinuclear iron complex of BPPFA analogous to (μ, η^2-BPPF)$Fe_3(CO)_{10}$ judging from the same color.[12] The spectral data provided in Tables 1 and 2 are all in a good agreement with the formulation of each compound. An interesting aspect to be noted concerning the coordination behavior of BPPFA is that in **2** this ligand acts as a monodentate through a single phosphorus like that shown in (η^1-BPPF)$Fe(CO)_4$, while in **3** it acts as a bridge employing both phosphorus atoms as seen in (μ, η^2-BPPF)$Fe_2(CO)_8$. This is evidenced by the presence of two ^{31}P signals and of the singlet for the free -NMe_2 group in each compound. Even more supportive is the ^{13}C-NMR pattern for the carbonyl groups as shown in Figure 1. Table 2 shows a doublet for the -$Fe(CO)_4$ moiety in **2** and a pair of doublets for the two non-equivalent -$Fe(CO)_4$ groups in **3**, Finally, an important question concerning the point of attachment of BPPFA in **2** can be answered by comparing both the ^{31}P and ^{13}C-NMR patterns of the three compounds **1-3**. Thus, for example, as shown in Figure 1., the chemical shift of the doublet at $\delta=212.8$ ppm in **2** is closer to that of the one at $\delta=212.9$ ppm which is arising from the -$Fe(CO)_4$ moiety attached to the -PPh_2 group in the singly substituted cyclopentadienyl ring in **3**.

Acknowledgment. TJK gratefully acknowledges the Korea Science and Engineering Foundation for the financial support (Grant No. 88-0304-03).

References

1. M. Kumada, T. Hayashi, and K. Tamao, *Fundamental Research in Homogeneous Catalysis*, Plenum Press, New York, p. 175 (1982).
2. T. Hayash and M. Kumada, *Acc. Chem. Res.*, **15**, 395 (1982).
3. W. R. Cullen, F. W. B. Einstein, T. Jones, and T. J. Kim. *J. Organometallics*, **2**, 741 (1983).
4. W. R. Cullen, F. W. B. Einstein, T. Jones, and T. J. Kim. *J. Organometallics*, **4**, 346 (1985).
5. T. G. Appleton, W. R. Cullen, S. V. Evans, T. J. Kim, and J. Trotter, *J. Organomet. Chem.*, **279**, 5 (1985).
6. T. J. Kim and K. C. Lee, *Bull. Korean Chem.*, **10**, 279 (1989).
7. T. Hayashi, M. Konishi, Y. Kobori, M. Kumada, T. Higuchi and K. Hirotsu, *J. Am. Chem. Soc.*, **106**, 158 (1984).
8. W. R. Cullen, S. V. Evans, N. F. Han, and J. Trotter, *Inorg. Chem.*, **26**, 514 (1987).
9. Y. Ito, M. Sawamura, and T. Hayashi, *J. Am. Chem. Soc.*, **108**, 6405 (1986).
10. Y. Ito, M. Sawamura, and T. Hayashi, *Tetrahedron Lett.*, **289**, 6215 (1987).
11. T. J. Kim, K. H. Kwon, S. C. Kwon, J. O. Baeg, S. C. Shim, and D. H. Lee, *J. Organomet. Chem.*, **389**, 205 (1990).
12. T. J. Kim, K. H. Kwon, S. C. Kwon, N. H. Heo, M. M. Teeter, and A. Yamano, Manuscript submitted for publication in Organometallics.
13. D. D. Perin, W. L. F. Armarego, and D. R. Perin, *Purification of Laboratory Chemicals*, 2nd ed., Pergamon press, New York, 1980.
14. T. Hayashi, T. Mise, M. Fukushima, M. Kagotani, M. Nagashima, Y. Hamada, A. Matsumoto, S. Kawakami, M. Konishi, Y. Yamamoto, and M. Kumada, *Bull. Chem. Soc. Jpn.*, **53**, 1138 (1980).
15. J. C. Kotz, C. L. Nivert, and J. M. Lieber, *J. Organomet. Chem.*, **84**, 255 (1975).

A Statistical Termodynamic Study of Phase Equilibria in Microemulsions

Kyung-Sup Yoo, and Hyungsuk Pak*

Department of Chemistry, Seoul National University, Seoul 151-742. *Received February 25, 1991*

To investigate the phase equilibria and structural properties of microemulsions, we study a simple phenomenological model on the basis of the cubic lattice cell with which the oil- and water-filled cells are connected one another, respectively. The surfactant is assumed to be insoluble in both oil and water, and to be adsorbed at the oil-water interface. The Schulman condition, according to which the lateral pressure of the surfactant layer is compensated by the oil-water interfacial tension, is found to hold to good approximation in the middle-phase microemulsion. Our results show that the oil- and water-filled domains in that microemulsion are about 50-150 Å across, and depend sensitively on the curvature parameters. The phase diagram is not symmetric in this model. It may be asymmetrized intrinsically by non-equivalency of oil and water. The two- and tree-phase equilibria including critical points and critical endpoints are found.

Introduction

Mixtures of oil and water are naturally unstable, but they can be stabilized by addition of suitable surfactants, which optimize their interactions by standing at the oil-water interface and decrease drastically the interfacial energy. With

small but finite interfacial tensions, oil-in-water and water-in-oil emulsions have rather large droplets (0.5-10 μm), and thermodynamically unstable.[1] However, some surfactants (or some surfactant mixtures: surfactant+cosurfactant) have a different behavior; unlike unstable macroemulsion systems, it is possible to reach a state of zero interfacial tension. A system of this sort tends to increase the total area of interface between oil and water. It is called a microemulsion, which was first described by Schulman.[2]

Microemulsions are thermodynamically stable oil-water-surfactant mixtures, sometimes containing salt and cosurfactant[3-6] as well. These systems have been extensively studied in recent years with relation to their practical applicabilities including tertiary recovery of oil deposits,[7] a possible low-emission fuel,[8] and a possible blood substitute.[9] Their structures have been studied with the help of various techniques such as small angle X-ray light scattering,[10] electron microscopy,[11] neutron scattering.[12] From a physicochemical viewpoint, microemulsions are of interest because they involve complex phase equilibria and critical phenomena. Three-phase equilibria[13-15] (a middle-phase microemulsion coexists with almost pure oil and water) and tricritical points[16-18] are examples.

Many theoretical studies are also processed and various models are proposed. There have so far been two different approaches to the construction of thermodynamic models for microemulsions. In this paper we follow the phenomenological approach[13,14,19] which was first initiated by Talmon and Prager,[19] and later further processed by de Gennes and coworkers.[20,21] Widom,[13] and Safran and coworkers.[14]

In most of previous papers[13,14,19] the free energy of mixing of oil and water is estimated by using the random-mixing approximation. But they did not consider the difference by non-equivalency of oil and water. Such models usually give a symmetrical phase diagram if the spontaneous curvature is not introduced. In this paper we use the random-filled approximation incorporating the molecular properties of oill, water and surfactant directly and indirectly, and so considering non-equivalency of oil and water. This shows the intrinsic asymmetry of phase diagram.

Theory

Model. Formally, the real system of microemulsions may be thought to have five independent chemical components (oil, water, surfactant, salt and cosurfactant), and so, at fixed temperature and pressure, one must consider four relevant thermodynamic variables. In this paper we consider microemulsions of ternary mixtures composed of oil, water and surfactant, likewise the model of Ref. (13). Our model, at fixed temperature and pressure, has thermodynamic variables of two chemical compositions ϕ_W and ϕ_O (volume fractions of oil and water), surfactant number density ρ (actually, some combination of the densities of surfactant and cosurfactant), and a geometrical lattice cell size variable ξ. The main role of the cosurfactant is to reduce the rigidity of the interfacial layer by making it flexible, and then to decrease the rigidity constant K and to modify the spontaneous radius ξ^o. In a real system of some surfactant one must see that the addition of salt is to give the change of spontaneous radius, and so, the water component is to be thought of as modeling brine.

With the above-mentioned assumptions, space is divided into cubes of an edge length ξ filled randomly either with water (probability ϕ_W) or with oil (probability ϕ_O). The sum of the volume fractions of oil and water is

$$\phi_O+\phi_W=1 \tag{1}$$

When two adjacent cells are filled differently, they are separated by an interface of area ξ^2. Therefore, the interfacial area per cell is

$$A=z\xi^2\phi_O\phi_W \tag{2}$$

where z (=6) is a coordination number of the cubic lattice. The number of surfactant molecules per cell is given by

$$n_S=N_S/N=N_S\xi^3/V=\rho\xi^3 \tag{3}$$

where N_S, N and V and total number of surfactant molecules, the total number of cells and the total volume of the system, respectively. From Eqs. (2)-(3), the interfacial area per surfactant molecule is obtained as

$$\sum=A/n_S=6\phi_O\phi_W/\rho\xi \tag{4}$$

Derivation of Free Energy. At first, we define the canonical partition function of the system and describe the total free energy, and later, we derive the detailed energy terms of the free energy. We assume that the oil- and water-filled cells are under the averaged environments, respectively.

The canonical partition function Q of the system is written as

$$Q=Q_{W/O}Q_{O/W}\exp(-W/kT) \tag{5}$$

where $Q_{W/O}$ and $Q_{O/W}$ are the partition function of the water-filled- W/O type cells (hereafter, we call them W/O cells) and the oil-filled- O/W type cells (hereafter, we call them O/W cells), respectively. The total average interaction potential energy W is

$$W=F_W^o+F_O^o+F_i+F_S+F_C \tag{6}$$

where F_W^o and F_O^o are the free energies of water- and oil-filled cells in the bulk phases, respectively. F_i, F_S and F_C are the energy of interaction of adjacent water- and oil-filled cells, the interaction energy by surfactant molecules which are constrained to stay at the oil-water interface, and the additional energy that arises from the deviation of the average curvature of the interfacial layer from some favored value, respectively.

The partition functions of W/O and O/W cells can be written as

$$Q_{W/O}=q_{W/O}^{N_{W/O}}\exp(-E_W/kT)/N_{W/O}!,$$

$$Q_{O/W}=q_{O/W}^{N_{O/W}}\exp(-E_O/kT)/N_{O/W}! \tag{7}$$

where $q_{W/O}$ and $q_{O/W}$ are the numbers of states of W/O and O/W cells, respectively. E_W and E_O are the average potential energies of W/O and O/W cells, respectively. $N_{W/O}$ and $N_{O/W}$ are the numbers of W/O and O/W cells, respectively. The formation of the W/O cell is related to the probability of having a band which favors concave toward water, and that of the O/W cells is related to the probability of having a band which favors convex toward water. Therefore, the num-

bers of *W/O* and *O/W* cells are assumed to be

$$N_{W/O} \simeq N\phi_W\phi_O^2,\ N_{O/W} \simeq N\phi_O\phi_W^2 \tag{8}$$

In consideration of mean-field approximation, the numbers of states of the *W/O* and *O/W* cells are written as

$$q_{W/O} = \Lambda_{W/O}^{-3} N_O \Delta v_O,\ q_{O/W} = \Lambda_{O/W}^{-3} N_W \Delta v_W \tag{9}$$

where $\Lambda_{W/O}$ and $\Lambda_{O/W}$ are the thermal de Broglie wave lengths of the *W/O* and *O/W* cell, respectively, and they are written as

$$\Lambda_j = h/(2\pi m_j kT)^{1/2} \tag{10}$$

where h, m_j, k and T are the Planck constant, the mass of j-species, the Boltzmann constant, and the absolute temperature (we use $T=300$ K in our calculations), respectively. In Eq. (9), N_O and N_W are the total numbers of oil and water molecules in the system, respectively, and they are written as

$$N_O = N\xi^3\phi_O/v_O,\ N_W = N\xi^3\phi_W/v_W \tag{11}$$

where v_O and v_W are the volumes per molecule of oil and water, respectively. In Eq. (9), Δv_O and Δv_W are the free volumes per molecule of oil and water, respectively. We use the physically reasonable values $v_O=325.5$ Å, $\Delta v_O=3$ Å^3,[22] $m_O=170.4$ g/mole (for decane), $v_W=29.9$ Å^3, $\Delta v_W=2$ Å^3,[22] and $m_W=18.0$ g/mole in our numerical calculations.

The thermodynamic equation for the Helmholtz free energy is

$$F = -kT\ \ln Q \tag{12}$$

From Eqs. (5)-(12), the total free energy of the system is rewritten as

$$F = -kTN\phi_W\phi_O^2\ \ln(\Lambda_{W/O}^{-3}\xi^3\Delta v_O e/v_O\phi_W\varphi_O) + E_W$$
$$-kTN\phi_O\phi_W^2\ \ln(\Lambda_{O/W}^{-3}\xi^3\Delta v_W e/v_W\phi_O\phi_W) + E_O$$
$$+F_W^\circ + F_O^\circ + F_i + F_S + F_C \tag{13}$$

The total free energy F can be given as the sum of five terms as follows:

$$F = F_P + F_e + F_i + F_S + F_C \tag{14}$$

(a) The first term is the sum of free energy of pure water F_W and pure oil F_O, that is

$$F_P = (E_W + F_W^\circ) + (E_O + F_O^\circ) = F_W + F_O \tag{15}$$

If f_W and f_O are the free energy densities of pure water and oil, respectively, then the free energy density of F_P becomes

$$F_{P,v} = (f_W\phi_W + f_O\phi_O) \tag{16}$$

This term has the same value in the system of separated oil and water phases, and in that of the microemulsions at given compositions, so it does not effect to the phase behaviors.

(b) The next contribution, F_e is the free energy of mixing entropy for a set of oil-filled cells which is mixed with a set of water-filled cells. In Eqs. (10) and (13), the thermal de Broglie wave length terms can be rewritten as

$$\Lambda_{W/O}^{-3} = (2\pi kTm_{W/O}/h^2)^{3/2} = (2\pi kTm_W n_W/h^2)^{3/2} = \Lambda_W^{-3}(\xi^3/v_W)^{3/2},$$
$$\Lambda_{O/W}^{-3} = (2\pi kTm_{O/W}/h^2)^{3/2} = (2\pi kTm_O n_O/h^2)^{3/2} = \Lambda_O^{-3}(\xi^3/v_O)^{3/2}, \tag{17}$$

where n_W $(=\xi^3/v_W)$ and n_O $(=\xi^3/v_O)$ are the numbers of oil and water molecules per cell, respectively. By using the relation of Eq. (17) and $V=N\xi^3$, the free energy density of F_e becomes

$$F_{e,m} = -(kT/\xi^3)\phi_W\phi_O^\gamma \ln[\Lambda_W^{-3}\Lambda v_O e(\xi^3/v_W)^{3/2}/\phi_W\phi_O]$$
$$-(kT/\xi^3)\phi_O\phi_W^\gamma \ln[\Lambda_O^{-3}\Lambda v_W e(\xi^3/v_O)^{3/2}/\phi_O\phi_W] \tag{18}$$

By this term, we can gain the intrinsic asymmetry of the phase diagrame.

(c) The third contribution, F_i is the energy of interaction of adjacent oil- and water-filled cells. If $\gamma_\circ$ is the interaction energy per unit area of contact, then F_i is written as

$$F_i = NA\gamma_\circ \tag{19}$$

We use a reasonable value $\gamma_\circ=50$ dyn/cm in our calculations. From the relation of $V=N\xi^3$ and Eq. (2), the free energy density of F_i becomes

$$F_{i,v} = 6\gamma_\circ\phi_W\phi_O/\xi \tag{20}$$

(d) The fourth term, F_S is interaction energy by the surfactant molecules which are constrained to stay at the oil-water interface. This term is proportional to the total number of surfactants. If $f_S(\Sigma)$ is the free enegry per surfactant molecule, then F_S can be written as

$$F_S = N_S f_S(\textstyle\sum) \tag{21}$$

If the surfactant in the interfacial layer behaves like a two dimensional ideal gas (in real systems, this problem is complicated by the possible presence of long range electrostatic interactions, repulsive interactions and interactions between surfactant and oil, and water, respectively), then from the surfactant interactions by an ideal gas type contribution[13] and the mean-field-like surfactant repulsions,[23,24] $f_S(\Sigma)$ can be expressed as

$$f_S(\textstyle\sum) = -kT\ \ln\sum + \sum_\circ^2 \gamma_\circ/\sum + g \tag{22}$$

where $\Sigma_\circ$ is the optimal surface area per surfactant molecule and g is the bulk free energy per surfactant molecule. We simply treat g as a function of temperature alone. In the saturated state Σ is close to $\Sigma_\circ$ to good approximation, then Eq. (22) is rewritten as

$$f_S(\textstyle\sum) = -kT\ \ln\sum + \sum_\circ\gamma_\circ + g = -kT\ \ln(\sum/\sum_T)$$
$$\textstyle\sum_T = \exp[(\sum_\circ\gamma_\circ + g)/kT] \tag{23}$$

From Eqs. (4), (21), (23) and the relation of $\rho=N_S/V$, the free energy density of F_S becomes

$$F_{S,v} = -kT\rho\ \ln(6\phi_W\phi_O/\xi\rho\textstyle\sum_T) \tag{24}$$

where Σ_T is a function dependent only on temperature. For convenience, we use $\Sigma_T=3.0$ Å^2 at $T=300$ K in our numerical calculations.

(e) The final term, F_C is the curvature free energy. This is the additional free energy that arises from any deviation of the average curvature of surfactant layer from the some favored value that reflects the geometry of the surfactant molecule and its interaction with the oil and water at two

surfaces of the layer. This curvature term is small, but cannot be omitted in the microemulsion systems where the interacial tension is very small, and it controls a detaile shape of the phase diagram. The curvature energy for the fluid interface has been described by Helfrich.[25] The curvature energy E_C is

$$E_C=K(c_1+c_2-2/r^\circ)^2/2 \tag{25}$$

where rigidity constant K represents the rigidity of the interface that determines the magnitude of the curvature free energy. The constants c_1 and c_2 are the local principal curvatures, and have the dimensions of the inverse length. The spontaneous radius r° characterizes the asymmetry of the layer. To apply these terms to the model, we substitute $1/\xi$ for c_1 and c_2, and ξ° for r°. Since this in an energy per surfactant molecule the curvature free energy of the system F_C can be written as

$$F_C=2KN_S(1-\xi/\xi^\circ)^2/\xi^2 \tag{26}$$

When the oil and water fractions are comparable the asymmetric effect by ξ° is of no consequence, and usually ξ° is larger than ξ. From the relation of $\rho=N_S/V$, the free energy density of F_C becomes

$$F_{C,v}=2K\rho[1-2\xi(\phi_O-\phi_W)/\xi^\circ]/\xi^2 \tag{27}$$

The parameter ξ° determimes a favored radius of curvature as that which minimizes F_C at fixed composition: $\xi=\infty$ (no curvature) when $(\phi_\circ-\phi_W)/\xi^\circ\leq 0$ [that is, when $\phi_O>\phi_W$ and $\xi^\circ<0$, or $\phi_O<\phi_W$ and $\xi^\circ>0$, and or $\xi^\circ=\infty$] or $\xi=\xi^\circ/2(\phi_O-\phi_W)$ when $(\phi_O-\phi_W)/\xi^\circ>0$. When $\phi_O>\phi_W$, positive ξ° favors *W/O* type curvature (concave to water), and vice versa when $\phi_O<\phi_W$, negative ξ° favors *O/W* type (convex to water).

Form Eqs. (16), (18), (20), (24) and (27), the total free energy density F_v becomes

$$\begin{aligned}F_v=&(f_W\phi_W+f_O\phi_O)\\&-(kT/\xi^3)\phi_W\phi_O^2\ln[\Lambda_W{}^3\Delta v_{Oe}(10j^3/v_O)(\xi^3/v_W)^{3/2}/\phi_W\phi_O]\\&-(kT/\xi^3)\phi_O\phi_W^2\ln[\Lambda_O{}^3\Delta v_{We}(10j^3/v_O)(\xi^3/v_O)^{3/2}/\phi_O\phi_W]\\&+6\gamma_\circ\phi_W\phi_O/\xi-kT\rho\ln(6\phi_W\phi_O/\xi\rho\textstyle\sum_T)\\&+2K\rho[1-2\xi(\xi_O-\phi_W)/\xi^\circ]/\xi^2\end{aligned} \tag{28}$$

In real systems the entropy of mixing is finite because the mixing cannot occur on a scale smaller than the sizes of the molecules themselves. Therefore, we can not use Eq. (28) itself to describe the system. We thus indroduce a as a microscopic cutoff length [13,14,20] and a has a typical intramolecular distance about 3-5 Å. We use $a=5$ Å in our model. In case of $\xi\geq a$ the total free energy F_v is given by Eq. (28), but $F_v=\infty$ when $\xi<a$, and so, we endow ξ with the minimum condition at $\xi=a$. This represents that we do not find the meaning for the system for which $\xi<a$.

Calculation of Free Energy. Figure 1 shows schematically the free energy density, F_v (ϕ, ρ; ξ) given by Eq. (28), as a function of ξ at fixed ϕ and ρ. The decreasing of the free energy density as ξ decreases toward to a is due to the factor $1/\xi^3$ in $F_{c,v}$ given by Eq. (18). At large value of ξ, the increasing of the free energy density as ξ increases is due to the term ln ξ in $F_{S,v}$ give by Eq. (24). In an intermediate range of ξ, as between ξ_x and ξ_n, the

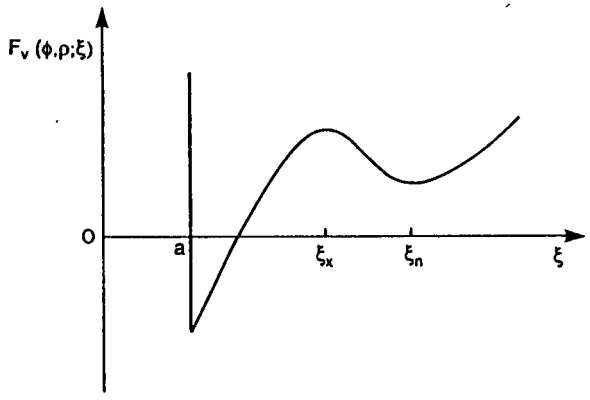

Figure 1. A schematic plot of F_v (ϕ, ρ; ξ) as a function of ξ at fixed ϕ, ρ. F_v (ϕ, ρ; ξ)$=+\infty$ at $\xi<a$. It has local minimum at $\xi=\xi_n$ and a local maximum at $\xi=\xi_x$.

free energy density decreases with increasing ξ. It is due to the factor $1/\xi$ in $F_{i,v}$ given by Eq. (20) and the factor $1/\xi^2$ in $F_{C,v}$ given by Eq. (27). The minimums at $\xi=\xi_n$ and a correspond to the stable microemulsion and almost pure oil or water phase at fixed ϕ and ρ, respectively.

The adsorption process of surfactant molecules on a planar oil- water interface at a fixed temperature can be described by the free energy of monolayer F_m. From Eqs. (19) and (21), F_m can be written as

$$F_m=F_i+F_S=NA\gamma_\circ+N_Sf_S(\textstyle\sum) \tag{29}$$

The first term of Eq. (29) represents the free energy of the bare oil- water interface and the second term correspond to the free energy of the monolayer. Then, from the relation of $NA=\Sigma N_S$, the free energy of the monolayer per surfactant molecule is

$$f_m(\textstyle\sum)=\sum\gamma_\circ+f_S(\sum) \tag{30}$$

The adsorbed surfactant molecules exert a lateral pressure

$$\Pi(\textstyle\sum)=-\partial f_S(\sum)/\partial\sum \tag{31}$$

which reduces the interfacial tension[20]

$$\gamma_m=\partial f_m(\textstyle\sum)/\partial\sum=\gamma_\circ-\Pi(\sum) \tag{32}$$

As the lateral pressure $\Pi(\Sigma)$ increases with decreasing Σ, at a particular $\Sigma=\Sigma^*$ the bare interfacial tension could, in principle, be precisely compensated by the lateral pressure leading to vanishing interfacial tension. And so, if F_i and F_S are the whole of the total free energy of the system, the minimum at ξ_n may occur where

$$\gamma_\circ-\Pi(\textstyle\sum^*)=0 \tag{33}$$

They call it the Schulman condition and refer to the state of the interfacial layer in which $\gamma_\circ=\Pi(\sum^*)$ as the saturate state.

From Eqs. (4), (23), (31) and (33), we can derive the cell size ξ_S by the Schulman condition and this may be a good approximation of ξ_n.

$$\xi_S=6\gamma_\circ\phi_O\phi_W/kT\rho \tag{34}$$

Because of other terms in the free energy F the condition Eq. (33) for the free energy minimum at $\xi=\xi_S$ does not hold exactly, but it does often hold with high accuracy.

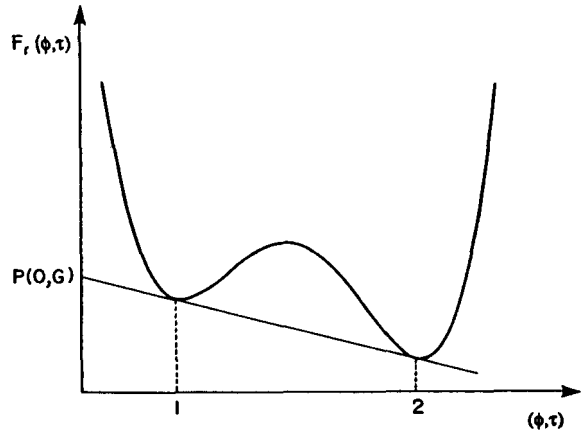

Figure 2. A schematic plot of F_r (ϕ, τ) as a function of two composition variables, ϕ and τ. The numbers 1 and 2 correspond to the stable two-phase equilibria.

We can define the reduced free energy as

$$\begin{aligned}F_r&=(a^3/kT)F_v\\&=(a^3/kT)[f_W\phi+f_O(1-\phi)]\\&-\phi(1-\phi)^2\ \ln[\Lambda_W^{-3}\Delta v_O e/a_W^{3/2}a_O)/\chi^3\\&-15\phi(1-\phi)\ \ln(\chi)/2\chi^3\\&+\phi(1-\phi)^2\ \ln[\phi(1-\phi)]/\chi^3\\&-\phi^2(1-\phi)\ \ln[\Lambda_O{}^3\Delta v_W e/a_O^{3/2}a_W)/\chi^3\\&+y\phi(1-\phi)/\chi-\tau\ \ln[\phi(1-\phi)/\textstyle\sum_r\tau\chi]\\&+K_r\tau[1-\chi\chi^\circ(1-2\phi)]/\chi^2\end{aligned}\tag{35}$$

where $\phi\equiv\phi_W$, and the dimensionles quantities χ, τ, a_j, y, K_r, χ° and Σ_r are given by

$$\chi=\xi/a\ \ (\chi\geq1),\ \ \tau=a^3\rho,\ \ a_j=v_j/a^3,\ \ y=6\gamma_o a^2/kT,$$
$$K_r=2K/a^2kT,\ \ \chi^\circ=2a/\xi^\circ,\ \ \textstyle\sum_r=\sum_T/6a^2\tag{36}$$

At fixed ϕ and ρ, by minimization of F_r the cell size is obaind from

$$\begin{aligned}&3\phi(1-\phi)^2\ \ln(\Lambda_W^{-3}\Delta v_O e/a_W^{3/2}a_O)+45\phi(1-\phi)^2\ \ln(\chi)/2\\&-15\phi(1-\phi)^2/2-3\phi(1-\phi)\ \ln[\phi(1-\phi)]\\&+3\phi^2(1-\phi)\ \ln(\Lambda_O^{-3}\Delta v_W e/a_O^{3/2}a_W)+y\chi^2\phi(1-\phi)\\&+\tau\chi^3-2K_r\tau\chi+K_r\tau\chi^2\chi^\circ(1-2\phi)=0\end{aligned}\tag{37}$$

From Eqs. (34) and (36), the approximation to χ_n ($=\xi_n/a$) which is given by the Schulman condition Eq. (33) is

$$\chi_n\simeq y\phi(1-\phi)/\tau\tag{38}$$

The holds when the terms $-yz^2\phi(1-\phi)$ and $\tau\chi^3$ are dominant in Eq. (37). In our numerical calculations we use the approximate χ_n [Eq. (38)]. It is very close to the exact τ_n from Eq. (37) if ϕ is not very small or large.

Conditions of Phase Equilibrium. The phase equilibria arise from concavities in the F_r (ϕ, τ) surface and are found by the common tangent construction.[21] In Figure 2, we let the common tangent plane on the F_r (ϕ, τ) surface. When the surface F_r (ϕ, τ) has singly tangent plane at one point, the coordinate of a point of single tangency is the composition of a single and stable phase. When a plane is simultaneously tangent to the surface at two points, the coordinates of two points of double tangency are the compositions of two stable and coexisting phases. Similarly, triple tangency gives three-phase equilibrium.

To obtain the coordinates of the points above the common tangent plane, we must know the common tangency from the F_r (ϕ, τ). As the chemical potentials of ϕ and τ, we find

$$\begin{aligned}\mu_\phi&=(\partial F_v/\partial\phi)_{\rho,\chi}=kT/a^3(\partial F,\partial\phi)_{\tau,\chi}\\\mu_\tau&=(\partial F_v/\partial\rho)_{\phi,\chi}=kT/a^3(\partial F,\partial\tau)_{\phi,\chi}\end{aligned}\tag{39}$$

At first, we multiply Eq. (39) by a^3/kT, and then subtract from μ_ϕ the physically inconsequential term $[a^3(f_W-f_O)/kT]$, and also subtract from μ_τ the equally arbitrary term [ln $(\Sigma_r e)$]. Thereby we define two thermodynamic dimensionless functions $L_\phi(\phi,\tau)$ for μ_ϕ and $L_\tau(\phi,\tau)$ for μ_τ which are given as

$$\begin{aligned}L_\phi(\phi,\tau)=&-(1-\phi)(1-3\phi)\ \ln(\Lambda_W^{-3}\Delta v_O e/a_W^{3/2}a_O)/\chi^3\\&-15(1-2\phi)\ \ln(\chi)/2\chi^3+(1-2\phi)\ \ln[\phi(1-\phi)]/\chi^3\\&+(1-2\phi)/\chi^3-\phi(2-3\phi)\ \ln(\Lambda_O^{-3}\Delta v_W e/a_O^{3/2}a_W)/\chi^3\\&+y(1-2\phi)/\chi-\tau(1-2\phi)/\phi(1-\phi)+2K_r\tau\chi^\circ/\chi\\L_\tau(\phi,\tau)=&-\ln[\phi(1-\phi)/\tau\chi]+K_r[1-\chi\chi^\circ(1-2\phi)]/\chi^2\end{aligned}\tag{40}$$

The conditions of phase equilibrium between a phase α at ϕ^α, τ^α and a phase β at ϕ^β, τ^β, are

$$L_\phi(\phi^\alpha,\tau^\alpha)=L_\phi(\phi^\beta,\tau^\beta),\ \ L_\tau(\phi^\alpha,\tau^\alpha)=L_\tau(\phi^\beta,\tau^\beta)\tag{41}$$

For three-phase equilibrium among phases α, β, and γ, we append the additional conditions $L_\phi(\phi^\beta,\tau^\beta)=L_\phi(\phi^\gamma,\tau^\gamma)$ and $L_\tau(\phi^\beta,\tau^\beta)=L_\tau(\phi^\gamma,\tau^\gamma)$ to Eq. (41). Here α and γ refer to almost pure oil or water phase, and β refers to the microemulsion phase. In Eq. (40), $\chi\equiv1$ in almost pure phases and $\chi\equiv\chi_n$ from Eq. (38) in the microemulsion phase.

The remaining condition of the pase equilibrium is as follows. From Figure 2, the coordinate of a point P at $\phi=0$ is (0, G) and at this point P, G is the value of F_r (ϕ, τ). We define the potential $G(\phi,\tau)$, Legendre transform of F_r (ϕ, τ), that is given as

$$G(\phi,\tau)=F_r(\phi,\tau)-\phi(\partial F_r/\partial\phi)_{\tau,\chi}-\tau(\partial F_r/\partial\tau)_{\phi,\chi}\tag{42}$$

The potential $G(\phi,\tau)$ has a common value G in all coexisting phases by a simple geometry. From Eqs. (35), (40) and (42), the defined function $H(\phi,\tau)$ for G (ϕ, τ) is written as

$$\begin{aligned}H(\phi,\tau)=&-\phi L_\phi(\phi,\tau)-\phi(1-\phi)^2\ \ln(\Lambda_W^{-3}\Delta v_O e/a_W^{3/2}a_O)/\chi^3\\&-15\phi(1-\phi)\ \ln(\chi)/2\chi^3+\phi(1-\phi)\ \ln[\phi(1-\phi)]/\chi^3\\&-\phi^2(1-\phi)\ \ln(\Lambda_O^{-3}\Delta v_W e/a_O^{3/2}a_W)/\chi^3\\&+y\phi(1-\phi)/\chi-\tau\end{aligned}\tag{43}$$

Therefore, the remaining condition of phase equilibrium between a phase α at ϕ^α, τ^α and a phases β, τ^β is

$$H(\phi^\alpha,\tau^\alpha)=H(\phi^\beta,\tau^\beta)\tag{44}$$

For three-phase equilibrium among phases α, β and γ, we append the additional condition $H(\phi^\beta,\tau^\beta)=H(\phi^\gamma,\tau^\gamma)$ to Eq. (44). Also in Eq. (43), $\chi\equiv1$ in almost pure phases and $\chi\equiv\chi_n$ from Eq. (38) in the microemulsion phase. For the α, β two-

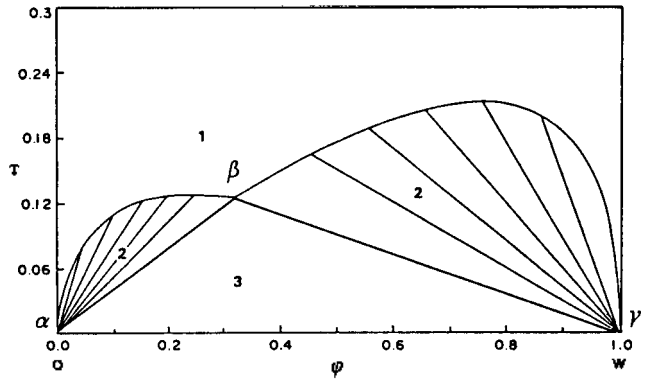

Figure 3. Phase diagram for $\chi^{\circ}=0.0$ and $K_r=2.0$. The numbers 1, 2, 3 indicate the number of coexisting phases, and the tielines in the two-phase regions are shown. Three one-phases are almost pure oil-phase (α), microemulsion phase (β) and almost pure water-phase (γ).

phase equilibria, there are four composition variables, ϕ^{α}, τ^{α}, ϕ^{β}, and τ^{β}, to be determined, and they give the coexistence curves that form the boundaries of the two-phase regions in the ϕ and τ plane, and all the tielines in that regions. For the three-phase equilibria, there are six composition variables, ϕ^{α}, τ^{α}, ϕ^{β}, τ^{β}, ϕ^{γ} and τ^{γ} which give the coordinates of three isolated points in the ϕ and τ plane, to be determined uniquely by the six equilibrium conditions.

Results and Discussion

Phase Diagrams. Figure 3 shows the phase diagram for $\chi^{\circ}=0.0$ and $K_r=2.0$, and here, one can see the asymmetry without considering the spontaneous curvature. The two invisible α, γ one-phase regions near $\tau=0$, $\phi=0$ and 1 on this scale show almost pure oil and water phases with the cell seze $\chi\simeq a$, respectively. The β phase arises from the $\chi\equiv\chi_n$ and it is a microemulsion phase. The αβ and βγ tielines in the two-phase regions along the boundaries of the phase diagram indicate the coexistence of the microemulsion phase with almost pure oil (phase α) and pure water (phase γ), respectively. The compositions of the α, β and γ phases in the three-phase equilibrium in Figure 3 are $\phi^{\alpha}=1.18\times10^{-4}$, $\tau^{\alpha}=2.89\times10^{-4}$, $^{\beta}=0.3203$, $\tau^{\beta}=0.1254$, $\phi^{\gamma}=0.9995$ and $\tau^{\gamma}=1.29\times10^{-3}$. The compositions ϕ^{α} and $1-\phi^{\gamma}$ are roughly the mutual solubility of water and oil in the α and γ phases. From Eq. (38), we calculate χ of the β phase in the three-phase equilibrium to be $\chi^{\beta}=31.42$. Thus, the model size of the middle-phase microemulsion is about 157 Å if we think of a as about 5 Å. This is reasonable size compared with the general experimental data.[10,26] From Eq. (37), we also can calculate the exact size at the same middle-phase composition to be $\chi^{\beta}=31.41$, which is nearly close to the size obtained by Eq. (38), so the Schulman condition Eq. (33) nearly holds in that microemulsion. If we extend the Schulman condition to the almost pure phases the cell sizes of α and β phases in the three-phase equilibrium are $\chi^{\alpha}\simeq\chi^{\gamma}\simeq1.48$, which nearly correspond to microscopic cutoff length a.

Effects of Curvature Parameters. Figures 4(a)-(c) show the asymmetric effect of phase diagrams for the change of spontaneous curvature [(a) $\chi^{\circ}=-0.05$, (b) $\chi^{\circ}=-0.01$ and (c) $\chi^{\circ}=0.03$] that characterizes the curvature of the surfactant layer at $K_r=3.0$. When χ° is negative [Figure 4(a)] the layer has the tendency of oill concave (*O/W* type), Winsor[27] type I region increases, and on the contrary when χ° is positive [Figure 4(c)], type II region increases. That is to say, as χ° increases (in real systems, increasing of the salinity) the composition ϕ, τ of the middle-phase moves at the near $\phi=1$ to the near $\phi=0$. This is denoted as type I-II-III transformation.[17] The oil-water symmertic phase diagram of $\chi^{\circ}=0.0$ in other papers[13,14] is similar to that of $\chi^{\circ}=-0.01$ [Figure 4(b)] in this paper. This represents that our model has the property of the more water concavity than others, and it

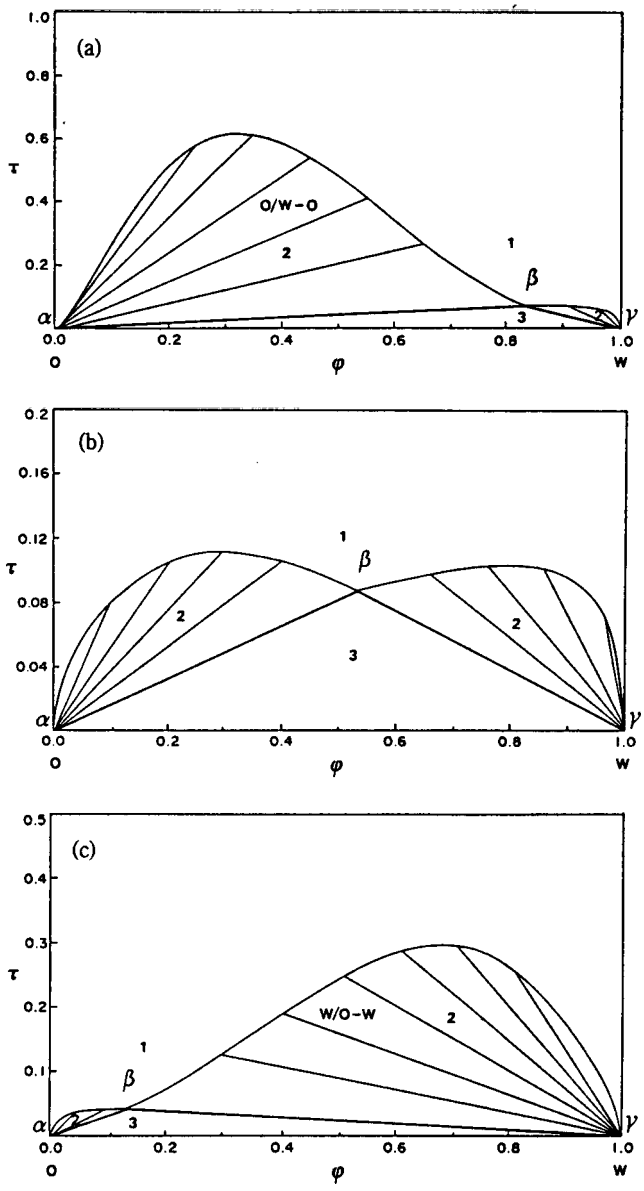

Figure 4. Phase diagram for $K_r=3.0$ at (a) $\chi^{\circ}=-0.05$, (b) $\chi^{\circ}=-0.1$ and (c) $\chi^{\circ}=0.03$. Three one-phases are almost pure oil-phase (α), microemulsion phase (β) and almost pure brine-phase (γ). The *O/W-O* and *W/O-W* indicate coexisting two-phase regions between *O/W*-type microemulsion and almost pure oil, and between *W/O*-type microemulsion and almost pure water, respectively.

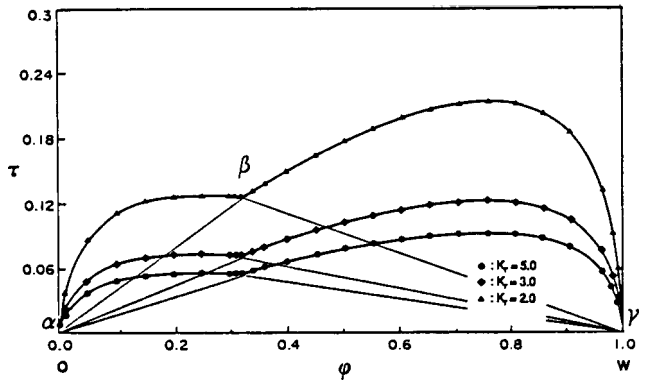

Figure 5. Phase diagram for $\chi^\circ = 0.0$ with the variation of K_r ($K_r = 5.0$, 3.0 and 2.0). Three one-phases are almost pure oil-phase (α), microemulsion phase (β) and almost pure water-phase (γ).

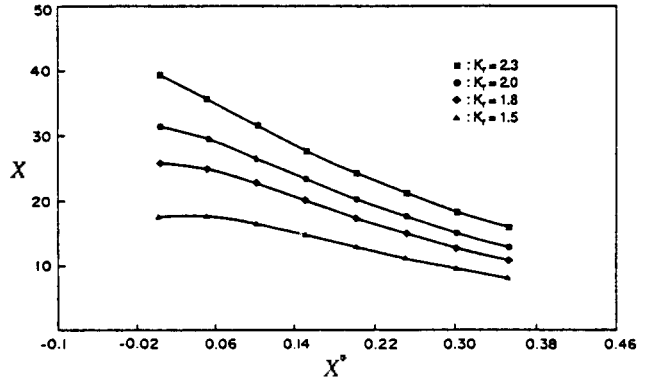

Figure 6. Cell size χ of the β phase in the three-phase equilibrium as a function of χ° with the variation of K_r ($K_r = 2.3$, 2.0, 1.8 and 1.5).

coincides with the tendency that *W/O* type microemulsion may be favored with small sizes than *O/W* type.[28] In Figures 4(a)-(c), the three-phase regions still exist. However, for large χ° the three-phase regions may vanish [one can see in Figure (8)]. Along the phase boundaries, ξ ($=\chi a$) scales with ξ° ($=2a/\chi^\circ$) indicates that the phase separation occurs when ξ is on the order of ξ°. This is an indication of the emulsification failure instability[19] that precludes the formation of cells with a size large than ξ°. In our model from the relation of $\chi^\circ = 2a/\xi^\circ$ in Eq. (36), when χ° is nearly -2.0 and 2.0 the three-phase equilibrium regions may disappear.

Figure 5 shows the changing effect of the phase digram with the variation of K_r at $\chi^\circ = 0.0$. At large K_r value the interface in very stiff. This means the decreasing of the total interfacial area, and so means the decreasing of the total adsorbing surfactant. In real system,[29] the microemulsion of a large K_r does not have cosurfactant or has only small quantity of cosurfactant. On the other hand at small K_r value by addition of some suitable cosurfactant, the interface is flexible and strongly wrinkled. this means the increasng of the interfacial area, and then the increasing of the total adsorbing surfactant. The results of this numerical calculations for the cell size of the β phase in the three-phase equilibrium at different K_r are $\chi^{\beta}_{K_r=5.0} = 72.17$, $\chi^{\beta}_{K_r=3.0} = 54.70$ and $\chi^{\beta}_{K_r=2.0} = 31.42$.

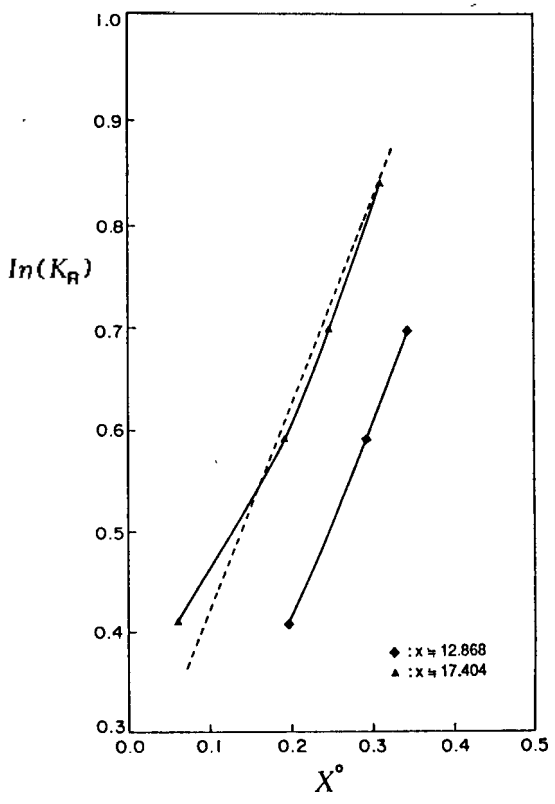

Figure 7. $\ln(K_r)$ as a function of χ° at different χ ($\chi = 12.868$ and 17.404). The dashed-straight line of $\ln K_r$ for χ° is $\ln K_r \simeq$ constant $+ 1.91\chi^\circ$.

Figure 6 shows the changing effect of the cell sizes of the middle phases for change of χ° with the variation of K_r value. Of course the relation of χ and K_r is the same as Figure 6, but the effect of K_r for the change of χ at various χ° show some difference. That is to say, that effect is larger-er at small χ°. This result shows that because the interfacial layer is less rigid at large cell length than small one, the layer of large cell length tends to bend easily even at a small spontaneous curvature.

The relation of K_r and χ° at the same cell sizes is shown in Figure 7, which is the plot of $\ln K_r$ for the change of χ° when cell sizes are $\chi = 17.404$ and 12.868. As to be expected even at Figure 6, the environment that gives the same cell size χ is that χ° increases with increasing of K_r. In our numerical calculation of such relation, we obtain the dashed-straight line of $\ln K_r$ for χ°, *i.e.*, $\ln K_r \simeq$ constant $+ 1.91\ \chi^\circ$. Likewise, we obtain the relation between χ of the middle phase and K_r at $\chi^\circ = 0.0$ and small K_r (it is reasonable and realistic in the microemulsion system.), *i.e.*, $\ln\chi \simeq -0.32 + 2.06K_r$. The two relation equations represent that the cell size always increases with decreasing χ° (increasing of ξ°) and increasing K_r, and so, it is very sensitive to the spontaneous radius and rigidity constant. At small K_r the decreasing of χ° may destabilize the stable microemulsion phase.

Phase Equilibria in Critical Regions. By this time we only considered the case of no spontaneous curvature ($\chi^\circ = 0.0$) or if any, of small curvature (from -0.05 to 0.03). We now consider the case of finite spontaneous curvature. Figure 8(a)-(c) show the change of phase diagrams as increasing the absolute value of χ° in the region of the γ phase

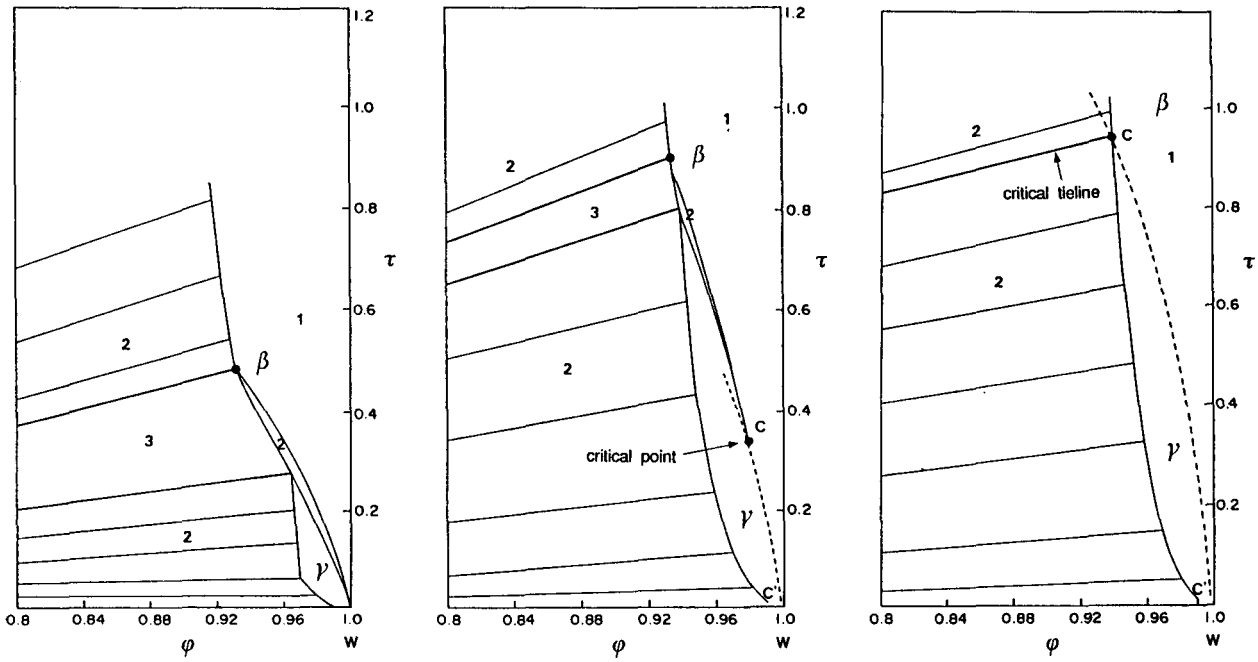

Figure 8. Phase diagrams in the region of water-rich phase for $K_r=3.0$ at (a) $\chi^\circ=-1.0$. (b) $\chi^\circ=-1.5$ and (c) $\chi^\circ=-1.82$. The numbers 1, 2, 3 indicate the number of coexisting phases. Two one-phases are microemulsion phase (β) and almost pure brine-phase (γ).

at $K_r=3.0$. For large enough χ°, that can affect profoundly the βγ phase equilibrium (water-rich side). Heavy lines are phase boundaries, light lines are tielines in the two-phase regions and the dashed lines indicate the surface of $\chi_r=1$ in Eq. (38). For $\chi^\circ=-1.0$, Figure 8(a) shows that the phase diagram is very distorted and the composition of the β phase in the three-phases equilibrium is $\phi^\beta=0.9328$, $\tau^\beta=0.4839$. For $\chi^\circ=-1.5$, Figure 8(b) shows that the βγ coexistence curve terminates at the point C on the dashed line, and the composition of a point C is $\phi_c=0.9810$, $\tau_C=0.3374$. In the small βγ coexistence region, $\xi^\beta\to a$ while $\xi^\gamma=a$ always, *i.e.*, $\xi^\beta\to\xi^\gamma$. The point C is the point at which there is no distinction between the β and γ phases, and is therefore a critical point. The dashed line C-C' has the same composition ϕ, τ and the same value a of their structural size ξ, and so the point C is called as a critical point and is also called as a tricritical point.[17,18] As χ° continues to increase negatively the three-phase triangle and the βγ two-phase region disappear. At the moment of their disappearance the critical point C and the β and γ vertices of the three-phase triangle coincide, while the βα and γα two sides of the triangle coincide and become a single tieline between the βγ critical phase and a coexisting α phase. Figure 8(c) shows the critical endpoint C and a critical tieline between the βγ critical phase at C and a coexisting α phase. Then the αβγ phase equilibrium is at its βγ critical endpoint. In our numerical calculations, the compositions of the point C and the endpoint of critical tieline in a coexising α phase are $\phi_C=0.9446$, $\tau_C=0.9467$, $\phi_C^\alpha=5.21\times10^{-6}$ and $\tau_c^\alpha=3.12\times10^{-9}$ at $\chi^\circ=-1.82$. On the other hand, the change of phase diagrams with increasing χ° in the region of the α phase shows the same tendency with decreasing χ° in the region of the γ phase. For large enough χ°, it can affect profoundly βα phase equilibrium (oil-rich side). For $K_r=3.0$ and $\chi^\circ=1.85$, the αβγ phase equilibrium is at the βα critical endpoint. In our numerical calculations, the compositions of the critical endpoint and the end point of critical tieline in the γ phase are $\phi_C=0.0491$, $\tau=0.8450$, $\phi_C^\gamma=0.99997$ and $\phi_c^\gamma=1.26\times10^{-8}$.

Conclusions

In this paper, we study a phenomenological model on the basis of the cubic lattice cell and show the intrinsic asymmetry of the phase diagram by non-equivalency of oil and water.

The Schulman condition is found to hold to good approximation is the middle-phase microemulsion, but it does not hold very well in the region of $\phi_O\phi_W\ll1$ by reason of other energy terms (in reality, these are important terms in describing microemulsions) besides the interfacial free energy terms.

The oil- and water-filled domains in the middle-phase microemulsion are about 50-150 Å and depend sensitively on the curvature parameters, rigidity constant K and spontaneous radius ξ°.

The relation between K and ξ° and the same cell size is found as $K\propto a^2kT\exp(3.82\ a/\xi^\circ)$.

Our model predicts three-phase equilibrium including a middle-phase microemulsion, and also shows the critical points and endpoints though it has some artificialities.

Acknowledgement. The present study was supported (in part) by the Basic Science Research Institute Program, Ministry of Education, Korea, 1990.

References

1. P. Becher, "*Emulsions: Theory and Practice*", 2nd ed., Reinhold, New York, Chap. 5 (1965).
2. J. H. Schulman and T. P. Hoar, *Nature*, **152**, 102 (1943).

3. E. Ruckenstein, *Soc. Ptrol. Eng. J. Oct.*, 593 (1981).
4. D. J. Mitchell and B. W. Ninham, *J. Chem. Soc. Faraday Trans. II*, **77**, 601 (1981).
5. A. M. Bellocq, J. Biais, P. Bothorel, D. Bourbon, B. Clin, P. Lalanne, and B. Lemanceau, in "*Microemulsions*", ed. by I. D. Robb, Plenum, New York (1982).
6. M. L. Robbins, in "*Micellization, Solubilization and Microemulsion*", ed. by K. L. Mittal, Vol. 2 (1977).
7. M. K. Sharma and D. O. Shah, "*Macro- and Microemulsions*", ed. by D. O. Shah, ACS Symposium Series 272 (1985).
8. S. E. Friberg and R. L. Vincent, in "*Encyclopedia of Emulsions Technology*", ed. by P. Becher, Vol. 1, Marcel Dekker, New York, (1983).
9. G. Mathis, P. Leempoel, J. Ravey, C. Selve, and J. Delpuech *J. Am. Chem. Soc.*, **106**, 6162 (1984).
10. D. Guest and D. Langevin, *J. Colloid Interface Sci.*, **112**, 208 (1986).
11. E. Sjöblom and S. E. Friberg, *J. Colloid Interface Sci.*, **67**, 16 (1978).
12. M. Kotlarchyk, S. H. Chen, J. S. Huang, and M. W. Kim, *Phys. Rev. A*, **29**, 2054 (1984).
13. B. Widom, *J. Them. Phys.*, **81**, 1030 (1984).
14. D. Alderman, M. E. Cares, D. Roue, and S. A. Safran, *J. Them,. Pays.*, **87**, 7229 (1987).
15. T. P. Stockfisch and J. C. Wheeler, *J. Pays. Them.*, **92**, 3292 (1988).
16. C. Borzi, R. Lipowsky, and B. Widow, in "*Microemulsion Systems*", ed. by H. L. Rosano and M. Clause, Surfactant Science Series, Vol. 24, Marcel Dekker (1987).
17. M. Barrel and R. S. Schechter, "*Microemulsions and Related Systems*", Surfactant Science Series, Vol. 30, Marcel Dekker (1988).
18. R. B. Griffiths, *Phys. Rev. B.*, **7**, 545 (1973).
19. Y. Talmon and S. Prager, *J. Chem. Phys.*, **69**, 2984 (1978).
20. P. G. de Gennes and C. Taupin, *J. Phys. Chem.*, **86**, 2294 (1982).
21. J. Jouffroy, P. Levinson, and P. G. de Gennes, *J. Physique*, **43**, 1241 (1982).
22. Y. Squeak, *J. Disp. Sci. Tech.*, **4**, 371 (1983).
23. J. N. Israelachvili, D. J. Mitchell, and B. W. Ninham, *J. Chem. Soc. Faraday Trans. II*, **72**, 1525 (1976).
24. M. Borkovec, *J. Chem. Phys.*, **91**, 6268 (1989).
25. W. Helfrich, *Phys. Lett.*, **43a**, 409 (1973).
26. L. Auvray, J. P. Cotton R. Ober, and C. Taupin, *J. Physique*, **45**, 913 (1984).
27. P. A. Winsor, *Chem. Rev.*, **68**, 1 (1968).
28. J. T. G. Overbeek, *Faraday Disse. Chem. Soc.*, **65**, 7 (1978).
29. J. M. di Meglio, M. Dvolaitzky, L. Leger, and C. Taupin, *Phys. Rev. Lett.*, **54**, 1686 (1985).